

## Research Report

# Rhes Suppression Enhances Disease Phenotypes in Huntington's Disease Mice

John H. Lee<sup>a,b</sup>, Matthew J. Sowada<sup>c</sup>, Ryan L. Boudreau<sup>c</sup>, Andrea M. Aerts<sup>d</sup>, Daniel R. Thedens<sup>e</sup>, Peg Nopoulos<sup>d</sup> and Beverly L. Davidson<sup>b,c,f,\*</sup>

<sup>a</sup>Medical Scientist Training Program, Roy J and Lucille A Carver College of Medicine, Iowa City, IA, USA

<sup>b</sup>Department of Molecular Physiology & Biophysics, Roy J and Lucille A Carver College of Medicine, Iowa City, IA, USA

<sup>c</sup>Department of Internal Medicine, Roy J and Lucille A Carver College of Medicine, Iowa City, IA, USA

<sup>d</sup>Department of Psychiatry, Roy J and Lucille A Carver College of Medicine, Iowa City, IA, USA

<sup>e</sup>Department of Radiology, Roy J and Lucille A Carver College of Medicine, Iowa City, IA, USA

<sup>f</sup>Department of Neurology, Roy J and Lucille A Carver College of Medicine, Iowa City, IA, USA

**Abstract.** In Huntington's disease (HD) mutant HTT is ubiquitously expressed yet the striatum undergoes profound early degeneration. Cell culture studies suggest that a striatal-enriched protein, Rhes, may account for this vulnerability. We investigated the therapeutic potential of silencing Rhes *in vivo* using inhibitory RNAs (miRhes). While Rhes suppression was tolerated in wildtype mice, it failed to improve rotarod function in two distinct HD mouse models. Additionally, miRhes treated HD mice had increased anxiety-like behaviors and enhanced striatal atrophy as measured by longitudinal MRI when compared to control treated mice. These findings raise caution regarding the long-term implementation of inhibiting Rhes as a therapy for HD.

**Keywords:** Huntington disease, Rhes, ras2, neurodegenerative disease, genetic therapies, RNA interference

Huntington's Disease (HD) is a fatal autosomal-dominant neurodegenerative disease caused by polyglutamine repeat expansion in exon 1 of huntingtin (HTT) [1]. Although the expression of mutant HTT (mHTT) protein is widespread, there is prominent degeneration in the caudate nucleus and putamen in HD brains. Recent cell culture studies reveal that a striatal-enriched protein, Rhes (Ras homolog enriched in striatum), was critical in mediating mHTT induced cytotoxicity. Rhes is a 266 amino acid GTP-binding protein and is expressed at high levels in the striatum during the postnatal period [2]. Rhes modulates dopamine D1 and D2 receptor sensitivity [3] and functions as an E3 ligase to enhance protein SUMOylation

[4]. In the striatum, Rhes expression is positively regulated by thyroid hormone [5]. Rhes is also a regulator of mechanistic target of rapamycin (mTOR) [6], a serine-threonine kinase that coordinates cell growth in response to environmental cues [7].

Rhes binds preferentially to mHTT over wildtype (WT) HTT [8]. This interaction induces SUMO1 conjugation of mHTT, and the presence of SUMO-modifiable lysines are necessary for Rhes-induced cytotoxicity in cell culture [8]. siRNA knockdown of Rhes in neuronal cell models expressing mHTT alleles improves cell survival [9, 10]. In addition, Rhes KO mice are resistance to 3-nitropropionic acid (3-NP)-induced lesions [11], and when Rhes KO mice were crossed to the R6/1 HD mice model, rotarod deficits were delayed [12]. Thus, current evidence suggests a toxic role of Rhes in causing striatal neuronal loss and behavioral deficits in HD. Therefore, it is important to

\*Correspondence to: Beverly L. Davidson, 200 Eckstein Medical Research Building, Department of Internal Medicine, University of Iowa, Iowa City, Iowa 52240, USA. Tel.: +1 319 353 5573; Fax: +1 319 353 3372; E-mail: beverly-davidson@uiowa.edu.

test approaches that reduce Rhes *in vivo* as a potential therapy.

To determine the *in vivo* disease relevance of Rhes, we used N171-82Q HD mice; they express the N-terminal fragment of mHTT previously shown to interact with Rhes and confer cytotoxicity *in vitro* [8]. If Rhes is a critical mediator of HD toxicity, reducing Rhes in N171-82Q mouse striata would be expected to improve disease phenotypes. We generated adeno-associated viruses (AAVs) that express inhibitory RNAs directed to Rhes using an artificial miRNA platform as described earlier [13]. Initial *in vitro* screening identified miRhes sequence 4 (miRhes) as a potent silencer of murine Rhes (Fig. 1A). Interestingly, transcriptional analysis showed basal Rhes levels were already reduced in N171-82Q mouse striata (Fig. 1B). To test for the beneficial effects of further Rhes reduction, AAVs expressing miRhes were injected into mouse striata. First, we evaluated knockdown efficacy and the efficiency of the viral delivery method. AAV.miRhes transduced greater than 90% of the striatal volume (data not shown), and potently reduced Rhes levels in WT and N171-82Q mice compared to control miRNA (AAV.miC) treated mice (Fig. 1B). To our surprise, we found that Rhes inhibition did not improve rotarod performance. AAV.miRhes treated N171-82Q mice performed poorly and similarly to control HD mice (AAV.miC and saline) at 14 and 18 weeks of age (Fig. 1C).

N171-82Q mice have a relatively short life span and may better model late stage disease [14]. In contrast, BacHD mice, which express full-length human mHTT, have slower disease progression and have a normal life span [15]. To test if Rhes suppression was better tolerated in this model, longitudinal behavioral and assessments of striatal atrophy were done. Similar to our findings in N171-82Q mice, Rhes suppression, which remained robust 10 months after AAV.miRhes injection (Fig. 2A), did not improve motor phenotypes (Fig. 2B). Interestingly, others' work has shown that Rhes KO mice show changes in volitional locomotion and anxiety-like phenotypes [2]. Consistent with this, AAV.miRhes-treated BacHD mice had reduced spontaneous locomotor activity and exploratory drive accompanied by increased anxiety-like behavior, compared to AAV.miC-treated mice (Fig. 2C–E). We also evaluated the effects of Rhes suppression on striatal volume longitudinally using small animal magnetic resonance imaging (MRI). We found that AAV.miRhes-treated BacHD mice showed an earlier onset of striatal atrophy compared to AAV.miC-treated mice (Fig. 2F). Cerebellar volumes were similar

among all groups and ages (Fig. 2G), as noted earlier [16].

In the present study, we used a viral-mediated approach to directly knockdown Rhes levels postnatally in the HD mouse striatum. Contrary to expectations based on prior work, we did not observe neuroprotection associated with Rhes suppression in two distinct transgenic HD mouse models. Rather, we found that prolonged Rhes suppression caused an early enhancement of striatal atrophy and in long-term studies, exacerbated behavioral deficits. These data imply a cytoprotective, rather than a cytotoxic role of Rhes in HD brain. In agreement with this, a recent report shows that Rhes is a positive regulator of autophagy in PC12 and HEK293 cells [17]. As autophagy has well-established beneficial effects on mHTT degradation [18, 19], inhibiting Rhes activity may have negative consequences in neurons. Rhes has also been found to regulate iron uptake into cells via PKA signaling, implying a potential role in maintaining brain iron homeostasis [20]. Furthermore, Rhes regulates mTOR signaling [6], which may play a critical role in governing fundamental cellular processes. Given this and that Rhes expression is already reduced in HD patient brain [21], we argue that loss of Rhes activity may contribute to HD phenotypes.

Our results contrast to a recent report showing that genetic deletion of Rhes delays the appearance of motor deficits in R6/1 mice [12]. While the observed differences may reflect the approaches used to reduce Rhes (postnatal knockdown versus developmental knockout) and different mouse models used, a consensus from ours and the prior study is that Rhes suppression does not rescue brain degeneration. In fact, Rhes KO mice demonstrate severe brain atrophy that is indistinguishable from R6/1 mice [12]. In addition, Rhes has been found to be a SUMO E3 ligase [8]. Enhancement of mHTT SUMOylation may be protective before disease onset but destructive in late stage HD when lysosomal activity is declined [22]. Whether Rhes may be cytoprotective in HD through activation of SUMOylation or other intracellular pathways *in vivo* remains to be determined.

Interestingly, Rhes KO mice are protected from striatal lesions caused by 3-NP, an older, rarely used chemical inducer of striatal pathology [11]. Given that the mHTT allele is not present when 3-NP is given to normal mice, the mechanism of neuron loss will likely be distinct from a setting where mHTT is present. Others have shown that Rhes enhances cell death in response to toxic environmental stimuli [23], and given the overlapping functions between Rhes and Rheb, it

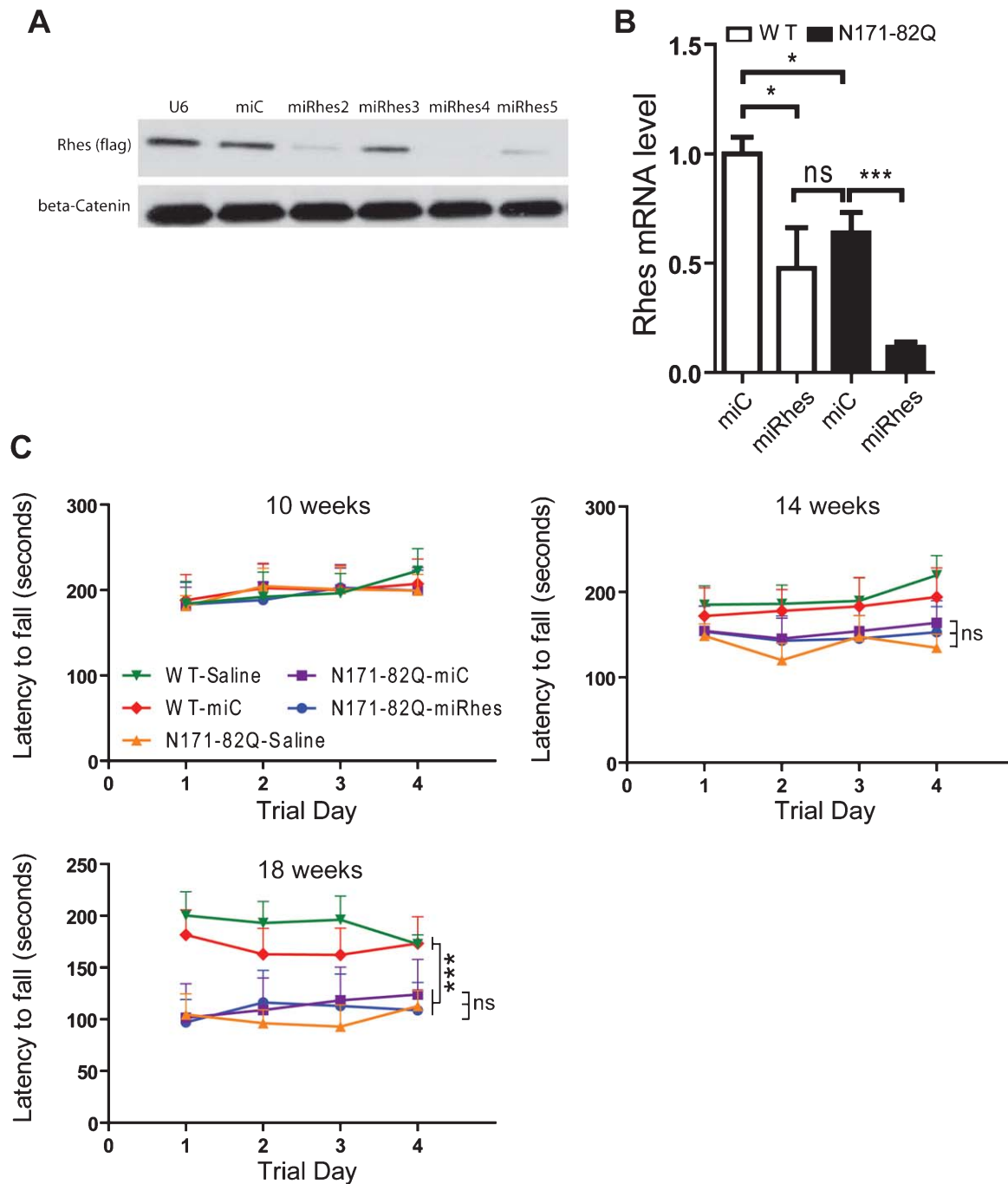


Fig. 1. Effects of Rhes suppression in N171-82Q mice. (A) miRhes2, miRhes4, and miRhes5 reduced Rhes protein expression 24h after co-transfection of Rhes-flag and miRNA-expressing plasmids into HEK293 cells. U6 is the miRNA promoter-only control. Rhes was detected by a flag antibody.  $\beta$ -catenin served as a loading control. (B) qPCR of striatal lysates from 19-week-old WT and N171-82Q mice treated with AAV.miC (WT: $N=11$ ;N171-82Q: $N=6$ ), and AAV.miRhes (miRhes4) (WT: $N=11$ ; N171-82Q: $N=6$ ) at 7 weeks of age. Rhes mRNA abundance was normalized to  $\beta$ -actin. Data represent mean  $\pm$  SEM. \* $P < 0.05$ ; \*\*\* $P < 0.001$ , One way ANOVA with Tukey post-hoc test. (C) Rotarod assessment of N171-82Q and WT mice after bilateral injection of saline, AAV.miC, AAV.miRhes at 7 weeks of age. Rotarod results from 10 weeks of age ( $N=5-9$  mice per group); 14 weeks of age ( $N=5-8$  mice per group); and 18 weeks of age ( $N=4-6$  mice per group). Rotarod data are shown as latency to fall (mean  $\pm$  SEM of trials 1-3 for each group per day). NS = Not statistically significant. Data represent mean  $\pm$  SEM. \*\*\* $P < 0.001$ , One-way ANOVA with Tukey post-hoc test.

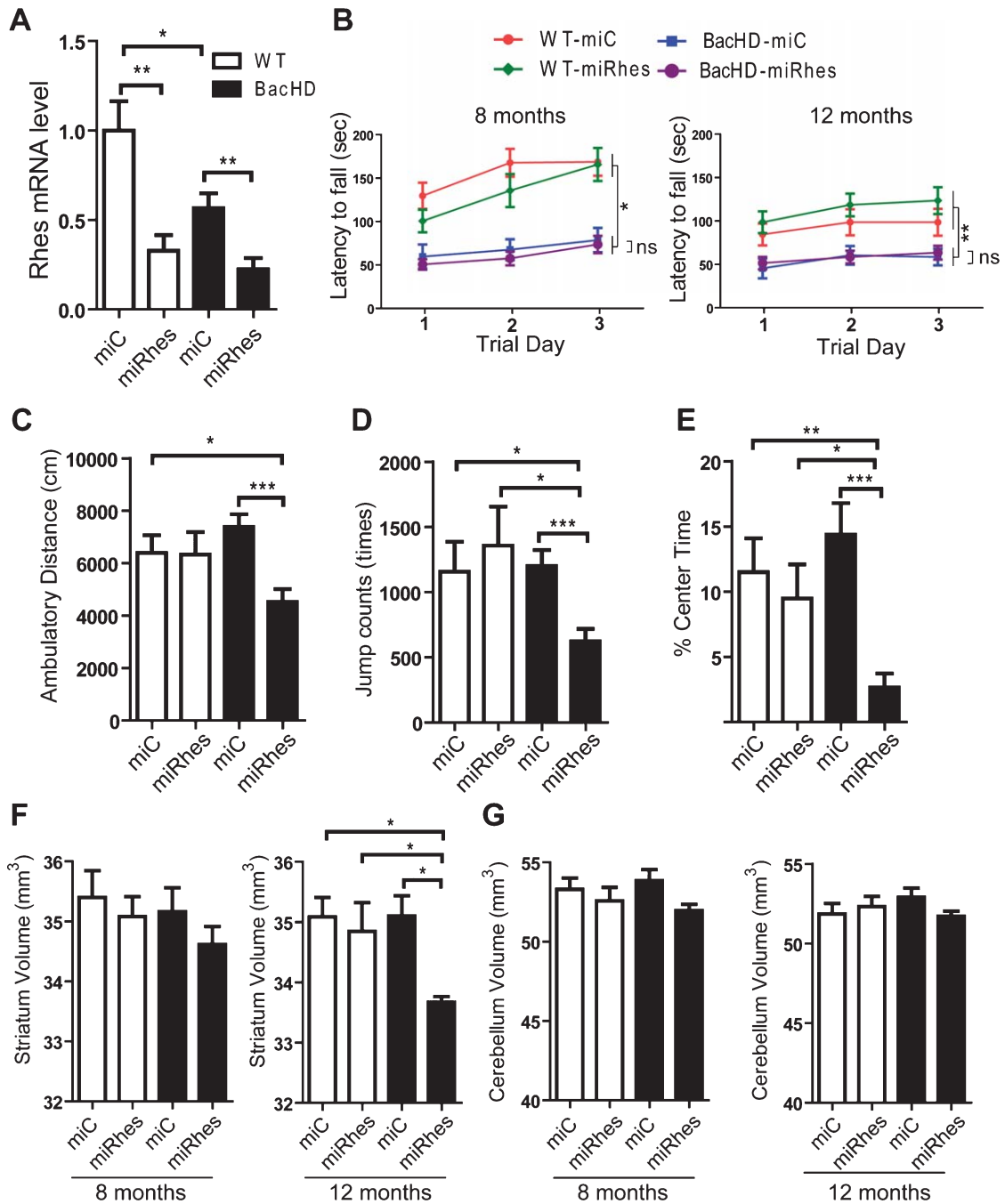


Fig. 2. Chronic Rhes suppression causes an early enhancement of disease phenotypes in HD mice. (A) qPCR analysis of Rhes in striatal lysates from 14-month-old WT and BacHD mice treated with AAV.miC (WT:  $N=6$ ; BacHD:  $N=5$ ) or AAV.miRhes (WT:  $N=6$ ; BacHD:  $N=7$ ).  $\beta$ -actin was used as an endogenous control. \* $P < 0.05$ , \*\* $P < 0.01$ , Student's t-test. (B) Rotarod assessment of BacHD and WT mice after bilateral injection of AAV.miC and AAV.miRhes into the striatum at 4 months of age. Rotarod at 8 months of age:  $N=14-16$  mice per group. Rotarod at 12 months of age:  $N=14-16$  mice per group. Rotarod data are shown as latency to fall (mean  $\pm$  SEM of trials 1-3 for each group per day). NS=Not statistically significant. Data represent mean  $\pm$  SEM. One-way ANOVA with Tukey post-hoc test. (C-E) Activity chamber analysis of locomotor and anxiety-like behavior for 12-month-old mice treated bilaterally with AAV.miC (WT:  $N=14$ ; BacHD:  $N=14$ ) or AAV.miRhes (WT:  $N=14$ ; BacHD:  $N=16$ ) at 4 months of age. \* $P < 0.05$ , \*\* $P < 0.01$ , \*\*\* $P < 0.001$ , One-way ANOVA with Tukey post-hoc test. (F and G) Longitudinal MRI assessment of striatal and cerebellar volumes in mice after bilateral AAV.miC (WT:  $N=8$ ; BacHD:  $N=7$ ) or AAV.miRhes (WT:  $N=7$ ; BacHD:  $N=8$ ) striatal injections at 4 months of age. Images were acquired at 8 and 12 months of age. \* $P < 0.05$ , One-way ANOVA with Tukey post-hoc test.

is plausible that normal levels of Rhes expression in wildtype mouse brain underlies the selective sensitivity of MSN to 3-NP toxicity. Consistent with this is the finding that several mHTT expressing HD mouse models show increased resistance to 3-NP and neurotoxin induced toxicity [24], possibly due to a lower basal level of Rhes. Thus, while Rhes may facilitate neuronal death in toxin exposure models or in cell culture, our study indicates a protective role for Rhes in the context of mHTT in brain. Collectively, these findings raise caution regarding long-term implementation of Rhes suppression in HD.

## MATERIAL AND METHODS

### *Animals*

All animal protocols were approved by the University of Iowa Animal Care and Use Committee. Mice were housed in a controlled temperature environment on a 12-hour light/dark cycle. Food and water were provided ad libitum. BacHD and N171-82Q mice were obtained from Jackson Laboratories (Bar Harbor, ME) and maintained on FVB/N and B6C3F1/J background respectively. Primers that specifically detect the human Htt transgene were used to genotype the mice. Age- and sex-matched wild-type mouse littermates were used for all behavioral studies.

### *Plasmids and AAV vectors production*

Artificial miRNA expression cassette was produced as described before [13]. Each artificial miRNA vector consisted of a RNA polymerase III mouse U6 promoter that drives siRNA expression (targeting endogenous murine Rhes or a scrambled control sequence). The siRNA sequences were screened to have low probability of targeting mouse 3'UTR [25]. The siRNA AAV shuttles also contained an eGFP gene under the control of the human cytomegalovirus immediate-early gene enhancer/promoter region. All the AAVs were produced by University of Iowa Vector Core, and AAV vectors serotype 1 (AAV1) were used. Real-time PCR was used to determine viral titers (miRhes:  $3 \times 10^{12}$  viral genomes/ml and miControl:  $3 \times 10^{12}$  viral genomes/ml).

### *Stereotaxic injection*

All mice were injected bilaterally into the striatum using the stereotaxic coordinates: 0.86 mm rostral to

bregma,  $\pm 1.8$  mm lateral to midline, 3.5 mm ventral to the skull surface. N171-82Q mice and WT littermates were injected with AAV.miRhes, AAV.miControl (AAV.miC), and saline at 7 weeks of age. BacHD mice and WT littermates were injected with AAV.miRhes and AAV.miC at 4 months of ages. Mice were injected with 5- $\mu$ l of vectors at an injection rates of 0.2  $\mu$ l/min.

### *Cell culture and transfections*

HEK293 cells were maintained in Dulbecco's modified Eagle's medium (Invitrogen) supplemented with 10% fetal bovine serum (Invitrogen). HEK293 cells were co-transfected with Rhes targeting miRNAs and/or pCMV-Rhes-flag plasmids using Lipofectamine 2000 (Invitrogen) as indicated by the supplier.

### *Quantitative real-time PCR (QPCR)*

RNA was isolated from striatal punches using TRIzol reagent. 500 ng of RNA was used for cDNA synthesis (High Capacity cDNA Reverse Transcription Kit; Applied Biosystems, Foster City, CA). Real-time PCR was performed using TaqMan 2x Universal Master Mix (Applied Biosystems). Taqman primer/probe set for Rhes (Mm04209172\_m1) was obtained from Applied Biosystem. Relative gene expression was calculated using the  $\Delta\Delta C_T$  method, normalizing to  $\beta$ -actin.

### *Behavioral assays*

#### *Accelerating rotarod*

The rotarod test was conducted as described previously [26]. Approximately equal number of male and female N171-82Q and BacHD mice were used for all behavioral studies. Baseline motor function for N171-82Q mice was acquired at 6 weeks of age, and then at 10, 14 and 18 weeks of age. BacHD mice baseline motor function was obtained at 4 months of age, and then at 8 and 12 months of ages. Before each test, mice were first habituated on the rotarod for 4 minutes and rested for at least one hour. Mice were tested for three trials per day and for 3 (BacHD) [27] and 4 (N171-82Q) [28] consecutive days as reported previously. After each trial, mice were allowed to rest for 30 minutes. For each trial, mice were placed on the rod that accelerates from 4–40 rotations per min over 4 minutes, and then speed maintained at 40 rpm. Latency to fall (or if mice hung on for two consecutive rotations without running) was used as a rating of motor performance. The trials were stopped at 300 seconds, and mice remaining

on the rotarod at that time were scored as 300 seconds. Data from the three trials for each group on each day are presented as means  $\pm$  SEM. Mice were always tested in the dark phase of the light/dark cycle. All of the behavioral experiments were conducted with the experimenter blind to mouse genotypes and treatments.

#### *Activity chamber*

Activity assay took place in a square arena (43.2  $\times$  43.2 cm) that comprised three planes of infrared detectors within a specially designed sound attenuating chamber (66  $\times$  55.9  $\times$  55.9 cm) under dim light (Med Associates, St Albans, VT). The animal was placed in the center of the testing arena and allowed to move freely while being tracked by an automated tracking system. The behavior data acquired during the first 10 min serves as an index of anxiety-like behavior. The locomotor activities were recorded over 30 min. All of the behavioral experiments were conducted with the experimenter blind to mouse genotypes and treatments. Single-time-point behaviors were compared using ANOVA. Tukey's post-hoc analysis was used to determine significance. In all cases,  $p < 0.05$  was considered significant.

#### *Magnetic Resonance Imaging (MRI) acquisition*

A 4.7 T small-bore MRI system (Varian, Inc., Palo Alto, California) was used to acquire T2-weighted MRI scans for BacHD mice at 8 and 12 months of ages at University of Iowa Biomedical Imaging Institute. The images were acquired with an in-plane resolution of 0.13  $\times$  0.25 mm<sup>2</sup> and an approximate slice thickness of 0.6 mm in the axial, sagittal, and coronal planes. Male mice from each treatment group were scanned using a standard structural imaging protocol designed to optimize the distinction between gray and white matter. All mice were fully anesthetized and intubated and oxygenated throughout the image acquisition. Post-imaging processing were done utilizing a mouse brain atlas, constructed from T2-weighted magnetic resonance microscopy images acquired from 11 normal female C57BL/6J mice. All of the experiments were conducted with the experimenters blind to mouse genotypes and treatments.

#### *Statistical analyses*

Data were analyzed using Student's t-test or One-way ANOVA analysis, followed by Tukey's post hoc analyses to assess for significant differences between

individual groups. All statistical analyses were performed by using GraphPad Prism version 5.0c. Data are expressed as mean  $\pm$  SEM. In all cases,  $P < 0.05$  was considered significant.

#### **ACKNOWLEDGMENTS**

The work was supported by Carver College Collaborative grant, NIH grants NS050568-03 (to PN), NIH grant NS0210 and NS076631 (to BLD) and the Roy J Carver Trust.

#### **CONFLICT OF INTEREST**

The authors have no conflict of interest to report.

#### **REFERENCES**

- [1] A novel gene containing a trinucleotide repeat that is expanded and unstable on Huntington's disease chromosomes. The Huntington's Disease Collaborative Research Group. *Cell*. 1993;72:971-83.
- [2] Spano D, Branchi I, Rosica A, Pirro MT, Riccio A, Mithbaokar P, Affuso A, Arra C, Campolongo P, Terracciano D, Macchia V, Bernal J, Alleva E, Di Lauro R. Rhes is involved in striatal function. *Mol Cell Biol*. 2004;24:5788-96.
- [3] Quintero GC, Spano D, Lahoste GJ, Harrison LM. The Ras homolog Rhes affects dopamine D1 and D2 receptor-mediated behavior in mice. *Neuroreport*. 2008;19:1563-6.
- [4] Subramaniam S, Mealer RG, Sixt KM, Barrow RK, Usiello A, Snyder SH. Rhes, a physiologic regulator of sumoylation, enhances cross-sumoylation between the basic sumoylation enzymes E1 and Ubc9. *J Biol Chem*. 2010;285:20428-32.
- [5] Vargiu P, Morte B, Manzano J, Perez J, de Abajo R, Gregor Sutcliffe J, Bernal J. Thyroid hormone regulation of rhes, a novel Ras homolog gene expressed in the striatum. *Brain Res Mol Brain Res*. 2001;94:1-8.
- [6] Subramaniam S, Napolitano F, Mealer RG, Kim S, Errico F, Barrow R, Shahani N, Tyagi R, Snyder SH, Usiello A. Rhes, a striatal-enriched small G protein, mediates mTOR signaling and L-DOPA-induced dyskinesia. *Nat Neurosci*. 2012;15:191-3.
- [7] Laplante M, Sabatini DM. mTOR signaling in growth control and disease. *Cell*. 2012;149:274-93.
- [8] Subramaniam S, Sixt KM, Barrow R, Snyder SH. Rhes, a striatal specific protein, mediates mutant-huntingtin cytotoxicity. *Science*. 2009;324:1327-30.
- [9] Lu B, Palacino J. A novel human embryonic stem cell-derived Huntington's disease neuronal model exhibits mutant huntingtin (mHTT) aggregates and soluble mHTT-dependent neurodegeneration. *FASEB J*. 2013;27:1820-9.
- [10] Seredenina T, Gokce O, Luthi-Carter R. Decreased striatal RGS2 expression is neuroprotective in Huntington's disease (HD) and exemplifies a compensatory aspect of HD-induced gene regulation. *PLoS One*. 2011;6:e22231.
- [11] Mealer RG, Subramaniam S, Snyder SH. Rhes deletion is neuroprotective in the 3-nitropropionic acid model of Huntington's disease. *J Neurosci*. 2013;33:4206-4210.
- [12] Baiamonte BA, Lee FA, Brewer ST, Spano D, LaHoste GJ. Attenuation of Rhes activity significantly delays the

- appearance of behavioral symptoms in a mouse model of Huntington's disease. *PLoS One*. 2013;8:e53606.
- [13] McBride JL, Boudreau RL, Harper SQ, Staber PD, Monteys AM, Martins I, Gilmore BL, Burstein H, Peluso RW, Polisky B, Carter BJ, Davidson BL. Artificial miRNAs mitigate shRNA-mediated toxicity in the brain: Implications for the therapeutic development of RNAi. *Proc Natl Acad Sci U S A*. 2008;105:5868-73.
- [14] Schilling G, Becher MW, Sharp AH, Jinnah HA, Duan K, Kotzuk JA, Slunt HH, Ratovitski T, Cooper JK, Jenkins NA, Copeland NG, Price DL, Ross CA, Borchelt DR. Intracellular inclusions and neuritic aggregates in transgenic mice expressing a mutant N-terminal fragment of huntingtin. *Hum Mol Genet*. 1999;8:397-407.
- [15] Gray M, Shirasaki DI, Cepeda C, Andre VM, Wilburn B, Lu XH, Tao J, Yamazaki I, Li SH, Sun YE, Li XJ, Levine MS, Yang XW. Full-length human mutant huntingtin with a stable polyglutamine repeat can elicit progressive and selective neuropathogenesis in BACHD mice. *J Neurosci*. 2008;28:6182-95.
- [16] Cheng Y, Peng Q, Hou Z, Aggarwal M, Zhang J, Mori S, Ross CA, Duan W. Structural MRI detects progressive regional brain atrophy and neuroprotective effects in N171-82Q Huntington's disease mouse model. *Neuroimage*. 2011;56:1027-34.
- [17] Mealer RG, Murray AJ, Shahani N, Subramaniam S, Snyder SH. Rhes, a Striatum-selective protein implicated in Huntington disease, binds beclin-1 and activates autophagy. *J Biol Chem*. 2013;
- [18] Ravikumar B, Vacher C, Berger Z, Davies JE, Luo S, Oroz LG, Scaravilli F, Easton DF, Duden R, O'Kane CJ, Rubinsztein DC. Inhibition of mTOR induces autophagy and reduces toxicity of polyglutamine expansions in fly and mouse models of Huntington disease. *Nat Genet*. 2004;36:585-95.
- [19] Yamamoto A, Cremona ML, Rothman JE. Autophagy-mediated clearance of huntingtin aggregates triggered by the insulin-signaling pathway. *J Cell Biol*. 2006;172:719-31.
- [20] Choi BR, Bang S, Chen Y, Cheah JH, Kim SF. PKA modulates iron trafficking in the striatum via small GTPase, Rhes. *Neuroscience*. 2013;253:214-20.
- [21] Hodges A, Strand AD, Aragaki AK, Kuhn A, Sengstag T, Hughes G, Elliston LA, Hartog C, Goldstein DR, Thu D, Hollingsworth ZR, Collin F, Synek B, Holmans PA, Young AB, Wexler NS, Delorenzi M, Kooperberg C, Augood SJ, Faull RL, Olson JM, Jones L, Luthi-Carter R. Regional and cellular gene expression changes in human Huntington's disease brain. *Hum Mol Genet*. 2006;15:965-77.
- [22] Steffan JS. Does Huntingtin play a role in selective macroautophagy? *Cell Cycle*. 2010;9:3401-13.
- [23] Karassek S, Berghaus C, Schwarten M, Goemans CG, Ohse N, Kock G, Jockers K, Neumann S, Gottfried S, Herrmann C, Heumann R, Stoll R. Ras homolog enriched in brain (Rheb) enhances apoptotic signaling. *J Biol Chem*. 2010;285:33979-91.
- [24] Zuchner T, Brundin P. Mutant huntingtin can paradoxically protect neurons from death. *Cell Death Differ*. 2008;15:435-42.
- [25] Boudreau RL, Spengler RM, Davidson BL. Rational design of therapeutic siRNAs: Minimizing off-targeting potential to improve the safety of RNAi therapy for Huntington's disease. *Mol Ther*. 2011;19:2169-77.
- [26] Boudreau RL, McBride JL, Martins I, Shen S, Xing Y, Carter BJ, Davidson BL. Nonallele-specific silencing of mutant and wild-type huntingtin demonstrates therapeutic efficacy in Huntington's disease mice. *Mol Ther*. 2009;17:1053-63.
- [27] Menalled L, El-Khodori BF, Patry M, Suarez-Farinas M, Orenstein SJ, Zahasky B, Leahy C, Wheeler V, Yang XW, MacDonald M, Morton AJ, Bates G, Leeds J, Park L, Howland D, Signer E, Tobin A, Brunner D. Systematic behavioral evaluation of Huntington's disease transgenic and knock-in mouse models. *Neurobiol Dis*. 2009;35:319-36.
- [28] Harper SQ, Staber PD, He X, Eliaison SL, Martins IH, Mao Q, Yang L, Kotin RM, Paulson HL, Davidson BL. RNA interference improves motor and neuropathological abnormalities in a Huntington's disease mouse model. *Proc Natl Acad Sci U S A*. 2005;102:5820-5.